

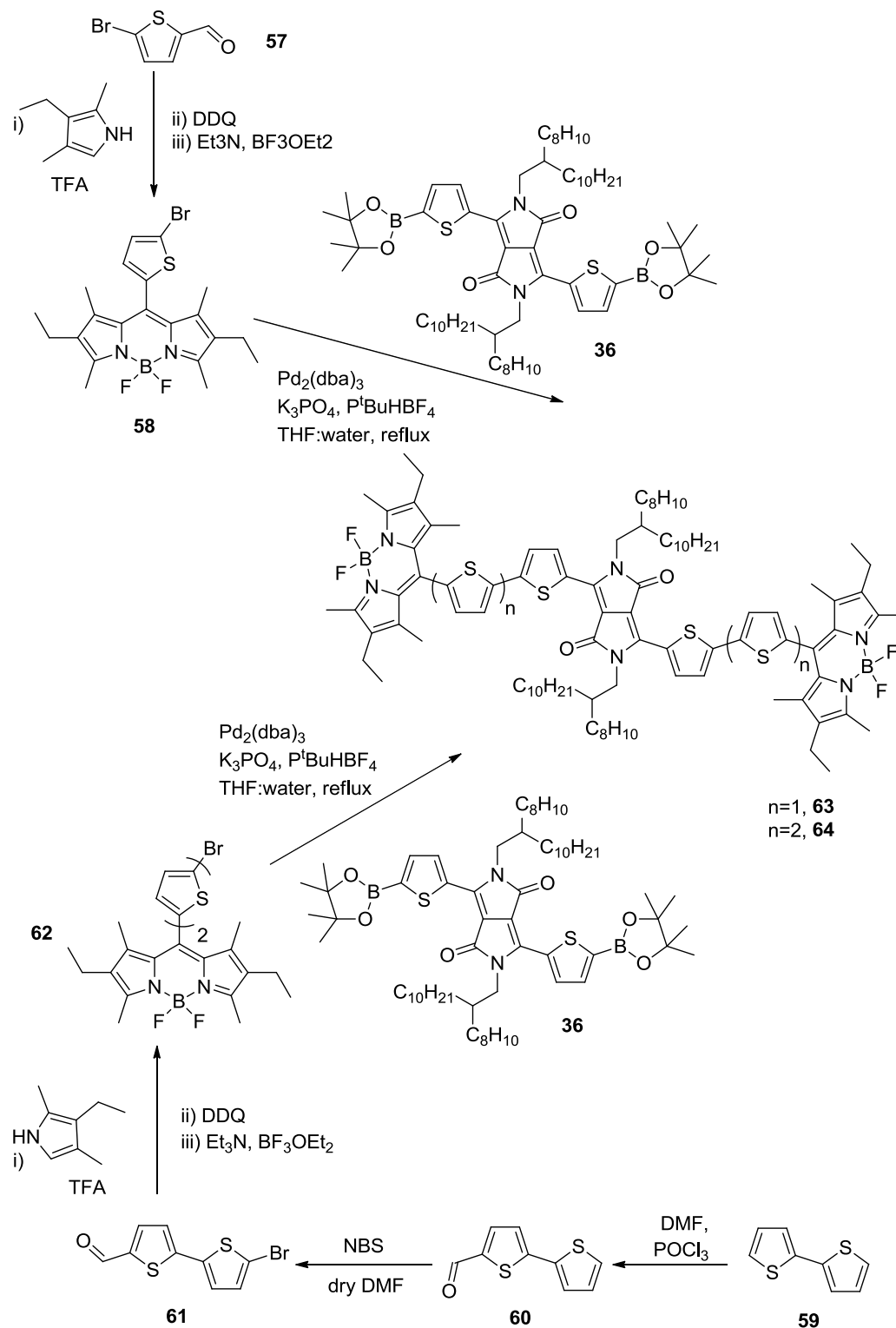
## **CHAPTER 4**

### *Synthesis of two Bodipy-DPP-Bodipy Triads for Organic Photovoltaics*

## 4.1. ABSTRACT

Due to the intrinsic problems of conjugated polymers, with reproducibility from batch to batch inconsistent, two new conjugated small molecules have been prepared to be studied in organic photovoltaics. In order to obtain a high range of photon harvesting, two well-known dyes, Bodipy and DPP, have been combined. The compounds, which are arranged in a triad approach (Bodipy-DPP-Bodipy), were obtained *via* Suzuki coupling. Full characterisation has been carried out for both triads. The characteristic absorption ranges of both units lies in different regions, so the combination is complementary and an increase in the absorption range has been observed.

## 4.2. SYNTHESIS



### 4.3. INTRODUCTION

Although previous works had been carried out to study the photovoltaic effects of organic compounds,<sup>1</sup> Tang *et al.* prepared the first organic solar cell (OSC) in 1975.<sup>2</sup> The device was fabricated by electrodeposition of microcrystalline chlorophyll-*a* **65** sandwiched between two metals with different work functions ( $M_1/\text{chl-}a/M_2$ ). The device showed a low power conversion efficiency (0.001 %), but demonstrated the possibility of using organic compounds in photovoltaic cells. Since then a vast number of organic compounds have been used as photoactive materials in the fabrication of organic solar cells.

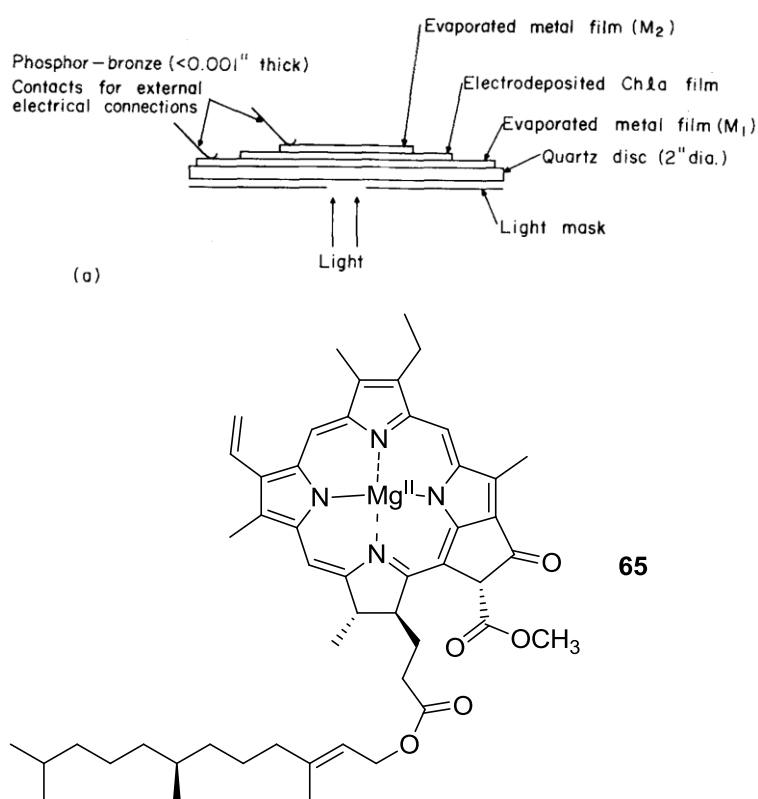


**Figure 4.1.** Schematic OPV device (above) and chlorophyll-*a* **65** (below).<sup>2</sup>

The first organic molecules that were investigated were small molecules such as tetracene, derivatives of merocyanine, phthalocyanine or porphyrins.<sup>1,3</sup> However, the discovery of efficient photoinduced electron transfer processes from conjugated

polymers to fullerene ( $C_{60}$ ) and the favourable interpenetrating network between them led to a major study of these systems.<sup>4,5</sup> The mechanical properties of conjugated polymers and their expected higher conductivities were also favourable to achieve good morphologies and therefore higher power conversion efficiencies. Nonetheless, in the middle of the last decade the interest for the small molecules has been revived. This interest derives from some of the advantages and properties that small molecules show over the conjugated polymers such as (i) the synthetic routes are usually shorter, (ii) higher structure versatility, (iii) purification and therefore reproducibility from batch to batch of the materials is well-defined, (iv) defined molecular weight, (v) they tend to form more ordered structures and (vi) they are more suitable to be used in different fabrication processes.

In order to obtain the best power conversion efficiency, both the properties of these compounds and the parameters of device fabrication (such as preparation techniques, thermal treatment, thickness of active layer, use of adequate electrodes or additives) have to be finely engineered. In terms of materials science, a control over the HOMO and LUMO level (and subsequently band gap), absorption range and coefficient and hole transport can be modified by relatively easy chemical modifications.

As a result of the growing number of OSCs fabricated from small molecules, the power conversion efficiency of these devices has recently exceeded the barrier of 5%.<sup>6,7,8,9</sup> Although the efficiencies are still lower than those obtained with polymeric systems, Heeger and co-workers have recently obtained a record of 6.7%.<sup>10</sup> The donor molecule is based on an A-D-A structure by attachment of two thiadiazolopyridine units to a central dithienosilole (**66**). The highest efficiency was obtained by spin coating a blend of the small molecule with PC<sub>70</sub>BM in a 7:3 ratio.

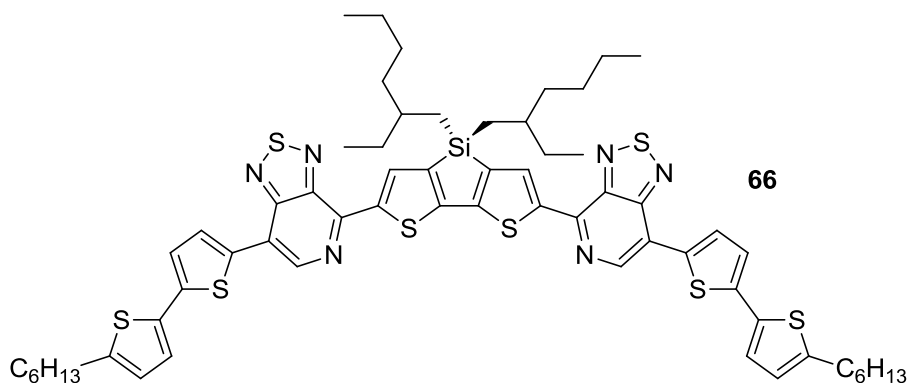


**Figure 4.2.** Chemical structure of **66**.

Small molecule compounds for OSCs have been mainly classified based on their chemical structure in some excellent reviews.<sup>11,12,13,14</sup> The majority of these small molecules used in OSCs can be considered as oligothiophenes, fused acenes, push-pull molecules or dyes. Oligothiophenes attracted much attention as they could be seen as the small relatives of the well-known P3HT. Roncali and co-workers synthesised some star shape triphenylamine and tetrahedral silane derivatives, which increased the dimensionality of the compounds, substituted with oligothiophenes.<sup>15,16</sup> Bauerle and co-workers obtained a maximum efficiency of 1.7 % with a highly branched oligothiophene dendrimer.<sup>17</sup> Nonetheless, the value of power conversion efficiency for oligothiophenes is still far below the best results obtained with P3HT. Interestingly, Skabara and co-workers have recently increased this value up to 2.26 % by coordinating oligothiophenes through a germanium centre (**67**).<sup>18</sup> It was observed by X-ray analysis that the spiro centre gives a cruciform arrangement that favours the  $\pi$ - $\pi$  stacking over 2D.

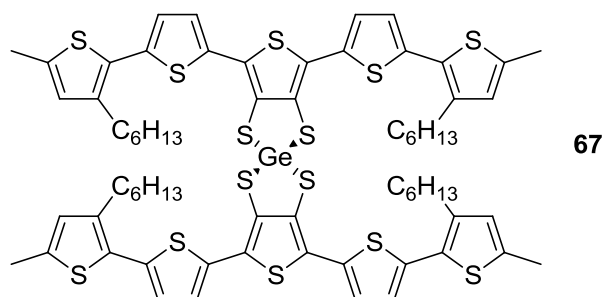


**Figure 4.3.** Chemical structure of **67**.

Soluble oligoacenes have also been used as donor materials in OSCs.<sup>11,12,13,14</sup> The fused ring system of these materials enables planar and crystalline structures and therefore high charge mobilities are expected. Starting with the early works of Maillaras and co-workers,<sup>19</sup> these materials have already surpassed a power conversion efficiency of 2%.<sup>20</sup> The main drawback of these compounds is the low ionisation potential (-4.9 eV) and due to the formation of large domains within the active layer, the interfacial area is reduced and therefore efficient exciton dissociation can be difficult.

The *push-pull* approach has been widely used in conjugated polymers.<sup>21</sup> This approach combines strong electron-donating moieties with electron-withdrawing moieties to obtain low band gap (HOMO-LUMO gaps for small molecules).<sup>16</sup> The light absorption of these molecules is enhanced by an intramolecular charge transfer (ICT) process occurring from the donor moiety to the acceptor moiety. Depending on the strength of the ICT process the absorptions can be pushed to the near infrared. Donors (D) such as triphenylamine or carbazole and acceptors (A) such as benzothiadiazole or dicyanovinylene are usually bridged by  $\pi$ -conjugated systems (e.g., thienyl, vinyl). There is not a fixed strategy to assemble the relative positions of the moieties within a molecule and therefore different combinations have been studied. The most common structures are D-A, A-D-A, D-A-D or combinations of these in branched arrangements. The aforementioned compound **66** has an A-D-A type structure and shows a broad band with a maximum at 655 nm (in chloroform) that can be ascribed to the ICT process.

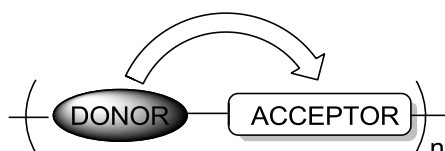


**Figure 4.4.** Donor-Acceptor approach.

In order to obtain high absorption coefficients and enhance the solar absorption, dyes have been used as *p* materials in OSCs. Dyes such as merocyanine,<sup>22</sup> squaraine,<sup>23</sup>

isoidindigo<sup>24</sup> and Bodipy<sup>25</sup> have been used recently. Bodipy derivatives are promising compounds to be used in the active layer as they show high absorption coefficients, good photostability and chemical robustness. Roncali *et al.* synthesised a series Bodipy derivatives (**68**, **69** and **70**) and their photovoltaic properties were studied.<sup>25,26,27</sup> In all these derivatives the fluorine atoms were replaced by ethynyl chains (the corresponding ethynyl Grignard derivative was used) to ensure low-lying HOMO energy levels. The presence of a second styryl derivative attached to the Bodipy core through the alpha position (**69**) increases the  $\pi$ -conjugated system and therefore the HOMO-LUMO gap decreases and the absorption shifts bathochromically. Compounds **68** and **69** were blended with PCBM in BHJ-structure OSCs and power conversion efficiencies of 1.17 and 1.34 % were obtained respectively.

In a later work, due to the appropriate HOMO and LUMO levels of both compounds as well as the complementary light-harvesting properties they show, Roncali and co-workers prepared an active layer bearing both dyes. Compounds **68** and **69** were blended together with PCBM to increase the power conversion efficiency of the OSCs made with single p-materials and PCBM up to 1.70 %.<sup>26</sup> This study showed clearly the possibility to enhance the efficiency of OSCs by mixing different donors within the active layer. In order to increase the hole-transport properties of the materials, an end-capped bis-thiophene unit was incorporated into the Bodipy on the *para* position of the phenyl ring.<sup>27</sup> Due to the non-planar conformation that the phenyl ring adopts with the Bodipy core, the influence of the bis-thionyl unit on the electronic properties is negligible. However, the increased degree of crystallinity of **70** over **69** gained by this modification can justify the higher power conversion efficiency obtained in OSCs (from 1.34% to 2.20%).

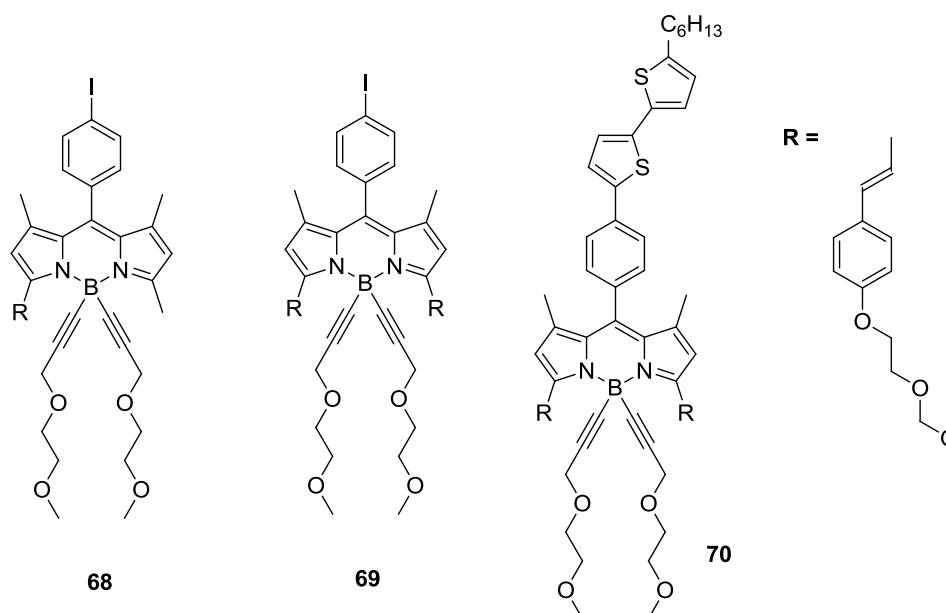


**Figure 4.5.** Series of BODIPY derivatives used in OPVs

Derivatives of the diketopyrrolopyrrole (DPP) pigment have also attracted the interest of the materials chemists in the last decade. DPP derivatives show high absorption coefficients and good photostability and they have been extensively copolymerised with a great number of donor moieties (thiophene, fused thiophenes, fluorene and carbazole among others) to obtain low band gap conjugated polymers.<sup>28</sup> The majority of these polymers show high ambipolar behaviour (hole and electron mobility) in OFETs and power conversion efficiencies over 5 % have been obtained in OSCs using them as *p*-materials.<sup>29</sup>

Likewise, small molecules based on DPP derivatives have been also synthesised and used for the fabrication of OSCs mainly by Nguyen and co-workers.<sup>30</sup> They first synthesised a series of DPP derivatives by addition of oligothiophenes on the 3 and 6 positions of the core **71**. The incorporation of these systems enlarged the conjugated backbone of the core and lowered the HOMO-LUMO gap of the molecules. By modifying wisely the substituents attached to the nitrogen atoms a power conversion efficiency of 3.0 % was obtained.<sup>31,32</sup> The power conversion efficiency of these types of derivatives was increased by attaching two benzofuran units to the dithieno-DPP core **72**.<sup>33</sup> The stabilisation of the HOMO level due to the presence of the benzofuran

units leads to an increase of the  $V_{OC}$  (0.92) and a power conversion efficiency of 4.4 % was obtained. Interestingly, whereas most of the focus is set on the development of new p materials for OSCs and the DPP derivatives (both small molecules and polymers) have been studied as such materials, Sonar and co-workers synthesised a series of DPP small molecules with n-type behaviour. A dithieno-DPP core was substituted with a series of electron withdrawing groups and blends of these with P3HT were studied in OSCs. The best results were obtained with compound **73** ( $\eta = 1\%$ ).

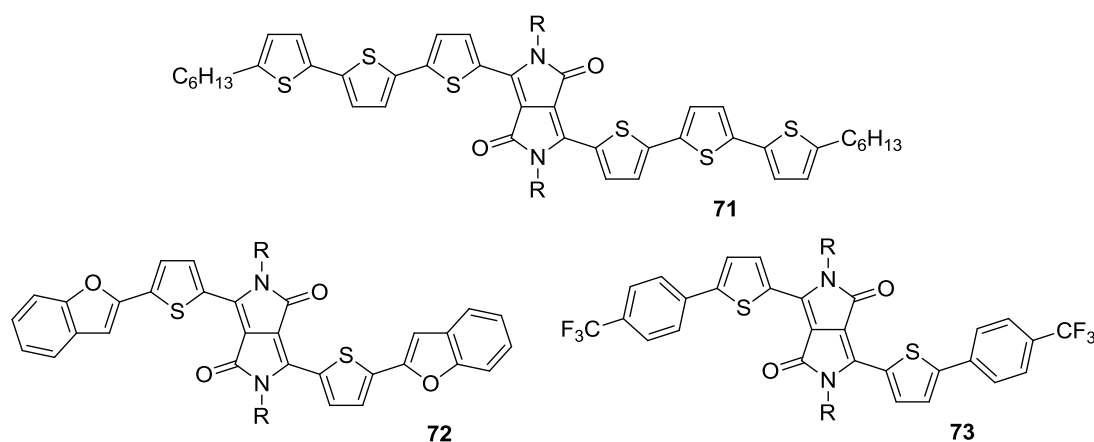


**Figure 4.6.** Series of DPP derivatives (**71-73**) studied in OPVs

#### 4.4. SYNTHESIS OF BODIPY-DPP-BODIPY TRIADS (**63-64**)

As it has been seen above, the use of derivatives of dyes has resulted in the fabrication of successful OSCs with power conversion efficiencies exceeding the barrier of 5%. Recently, in Skabara's group Bodipy and DPP cores have been incorporated successfully into conjugated polymers which have been used as *p*-type materials for the fabrication of OSCs. Attracted by the interesting properties that small molecules show over conjugated polymers and interested in understanding the effect of combining two different dyes into the same compound, a series of Bodipy and DPP derived compounds have been synthesised. Do the properties of Bodipy

and DPP cancel or combine with each other, or on the other hand they act independently?

To the best of our knowledge, there is one study in which Bodipy and DPP have been incorporated into a single molecule. Ziessel and co-workers synthesised a series of dyads and triads with a DPP core which was mono- or di-substituted with Bodipy derivatives and linked by a bis-phenyl-ethynyl bridge (**74**).<sup>34,35</sup> It was demonstrated that the electronic energy transfer in the triads can be switched effectively by protonation of one of the Bodipy derivatives.

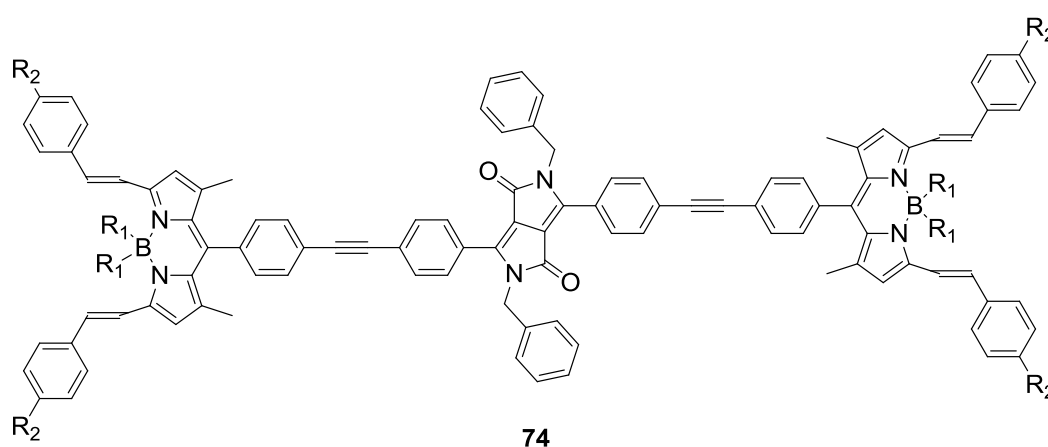
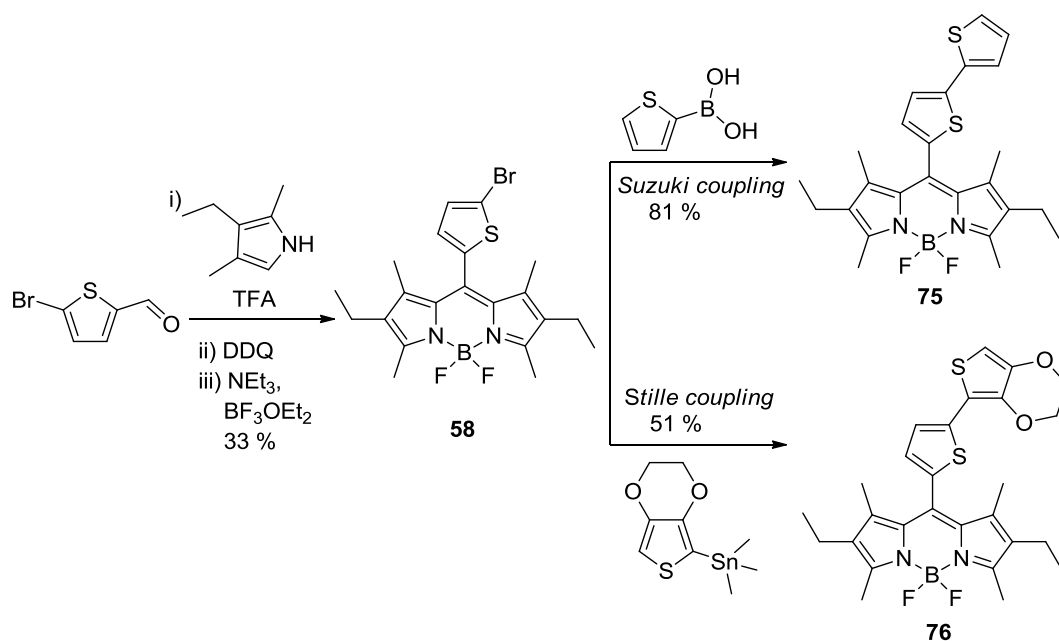


**Figure 4.7.** Triad based on a BODIPY-DPP-BODIPY **74**.

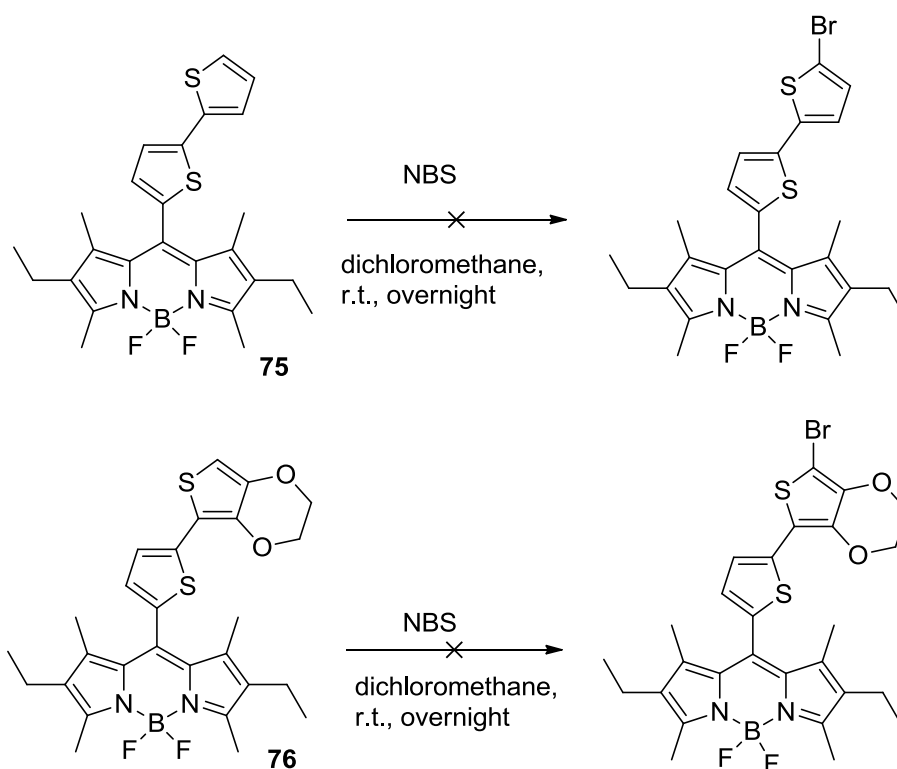
The bis-boronate DPP derivative **36** (see chapter 3) has been demonstrated to be a suitable intermediate to prepare DPP derivatives when obtaining the boronic ester derivative of the other coupling unit is not easy to obtain. Thus, the synthetic approach was focus on preparing Bodipy derivatives bearing brominated thiophene or EDOT units on the *meso*-position and coupled these derivatives *via* Suzuki coupling to the central DPP core. Compound **58** was prepared by acidic catalysis condensation of 5-bromothiophene-2-carbaldehyde with 3-ethyl-2,4-dimethylpyrrole and followed by oxidation with DDQ. Deprotonation with triethylamine and subsequent treatment with boron trifluoride diethyl etherate yielded **58**. The entire synthesis was carried out in one-pot.



**Scheme 4.1.** Synthesis of Bodipy derivatives **58**, **75** and **76**.

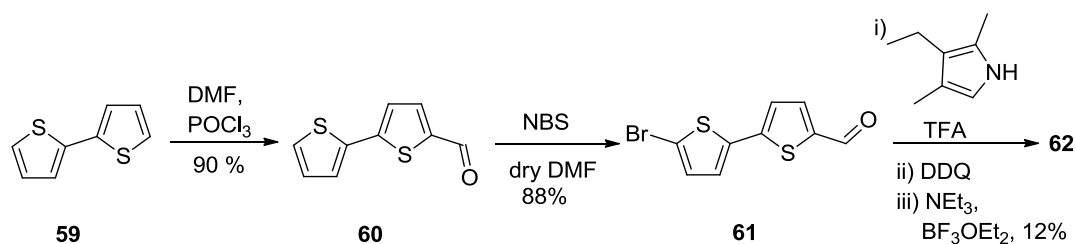
The extension of the conjugated  $\pi$ -system leads to compounds with lower HOMO-LUMO gaps and bathochromic shifts of the absorption spectra. Both effects are desirable to enhance the solar absorption. Therefore, the conjugation system of compound **58** was extended by incorporating an extra thiophene ring (**75**) and an EDOT unit (**76**). It has been shown that the attachment of thiophene units to Bodipy derivatives increase the hole mobility of these compounds.<sup>27</sup> Likewise, the incorporation of an EDOT unit should give a higher degree of planarity to the compound, which can be beneficial for obtaining close molecular interactions in the active layer and therefore the mobility of the charges.

Compound **58** was reacted with thiophene-2-boronic acid *via* Suzuki-Miyaura cross-coupling reaction to yield compound **75**. On the other hand, compound **76** was obtained by reacting **58** with stannylated-EDOT *via* Stille coupling. Both couplings work relatively well. In order to obtain halogenated derivatives to be cross-coupled with **36**,  $\alpha$ -bromination of both the thionyl and EDOT units was then tried. Compounds **75** and **76** were reacted with *N*-bromosuccinimide (NBS, 1.1 eq). Although the starting material was practically completely consumed, no signal of the desired brominated Bodipy derivatives was achieved (see Scheme 4.2).



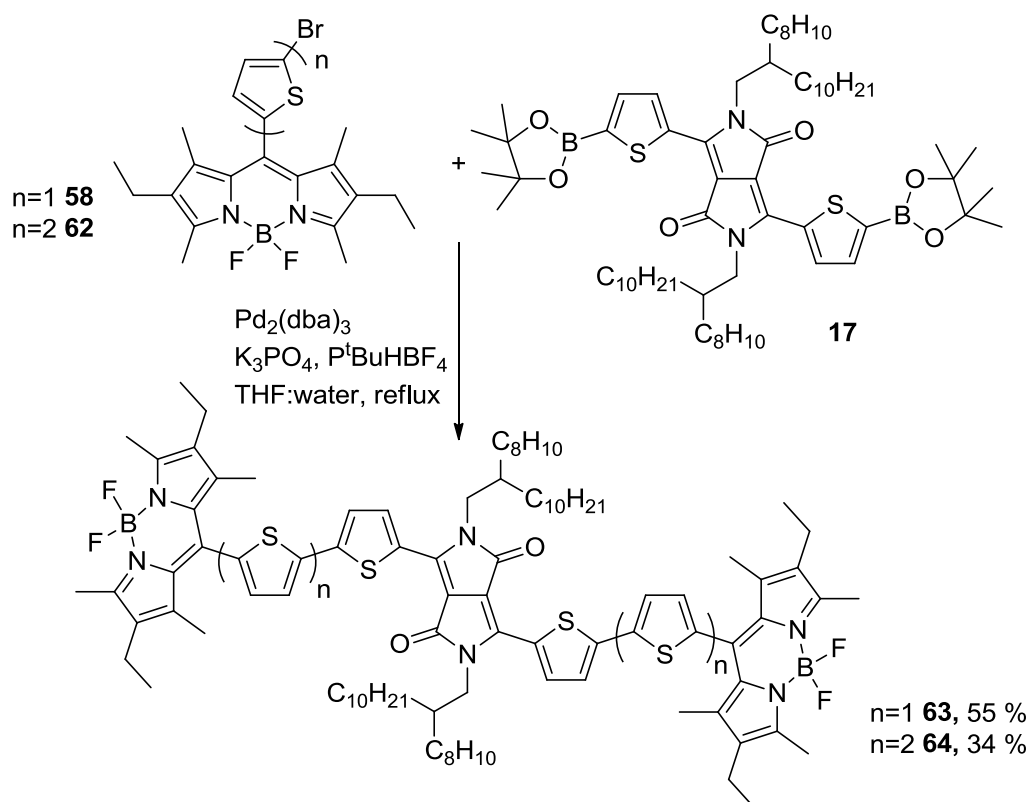
**Scheme 4.2.** Synthesis of brominated Bodipy derivatives.

Due to the unsuccessful approach followed to prepare the Bodipy bearing a brominated bis-thiophene unit on the *meso*-position, an alternative route to prepare these compounds was followed. The synthesis of **62** was achieved from the  $\alpha$ -brominated derivative of a bis-thionyl carbaldehyde (**61**). This synthetic route to prepare **62** has been already described in the literature.<sup>36</sup> Formylation of bis-thiophene was carried out *via* Vilsmeier-Haack by treatment with phosphorous oxychloride and *N,N*-dimethyl-formamide (**60**). Compound **60** was brominated with NBS (1.05 eq.) to yield compound **61**. Both steps proceed in high yields with an overall yield of ~80% (90% for the formylation and 88% for the bromination, respectively). Compound **62** was prepared following the same procedure as was used to synthesise **58**. Whereas the synthesis of **58** was achieved in 33%, the yield decreased to ~12% when the derivative with two thiophenes was prepared. However, both yields are similar to those reported in the literature for the same compounds.



**Scheme 4.3.** Synthesis of **62**.

The Bodipy-DPP-Bodipy triads (**63** and **64**) were synthesised *via* Suzuki-Miyaura cross-coupling reaction (Scheme 4.4.). The functionalised DPP core was reacted with the brominated Bodipy derivatives **58** and **62** in THF using  $\text{Pd}_2(\text{dba})_3$  and  $\text{K}_3\text{PO}_4$  as catalyst and the base, respectively. Several chromatographic columns and precipitations were required to isolate the triads from the crude mixture (see Experimental section). A further purification step using HPLC was required to isolate compound **64** in high purity.



**Scheme 4.4.** Synthesis of triads **63** and **64**.

## 4.5. ELECTROCHEMICAL AND OPTICAL PROPERTIES OF BODIPY-DPP-BODIPY TRIADS (63-64)

The electrochemical behaviour of the Bodipy-DPP-Bodipy triads (**63** and **64**) was determined by cyclic voltammetry analysis both in solution (0.1 mM of **63** or **64** in dichloromethane) and in the solid state with *iR* compensation. The experiments were carried out at a scan rate of 0.1 V/s. Ag wire, Pt wire and a glassy carbon electrode were used as the reference electrode, counter-electrode and working electrode, respectively. In solid-state experiments a film of **63** and **64** was drop-cast onto the working electrode from a dichloromethane solution. The experiments were carried out using tetrabutylammonium hexafluorophosphate (0.1 M) as the supporting electrolyte and all the values are quoted *versus* the redox potential of the ferrocene/ferrocenium couple. The oxidation and reduction graphs for each experiment were obtained independently and not as a full cycle, as the presence of irreversible peaks can give imprecise redox behaviours. Additionally, the solutions were bubbled with argon prior to each reduction process.

The oxidation and reduction processes of **63** and **64** in solution are shown in Figure 4.8. and Table 4.1. depicts all the electrochemical data. Upon oxidation, **63** shows two reversible peaks at +0.42 and +0.83 V and **64** shows three reversible processes at +0.37, +0.57 and +0.73 V. In both cases, the first oxidation wave can be assigned to the formation of the radical cation on the terthiophene-DPP part of the molecule. The lower oxidation potential for **64** compared to **63** is consistent with the tendency to decrease the oxidation potential when the oligothiophene chain is extended.<sup>37</sup> The second oxidation wave in **63** and the third in **64** can be ascribed to the oxidation of the Bodipy core. The second process in **64** can be assigned to the formation of the radical dication due to the presence of two additional thiophene rings compared to **63**.

The reduction processes of the triads are complicated to interpret properly due to the multiple reduction processes occurring. Compound **63** shows one quasi-reversible peak at -1.48 V, one reversible peak at -1.58 V and one irreversible peak at -2.01 V.

The reduction behaviour of **64** is more complex as several processes are overlapping. Compound **64** displays three quasi-reversible peaks at -1.48, -1.55 and -1.90 V and an irreversible peak at -2.09 V. It is adventurous to assign accurately each of these processes, but undoubtedly the first two reduction processes are due to the reduction of the DPP and Bodipy moieties. The reduction waves at higher negative potentials can be due to the reduction of the oligothiophene units.

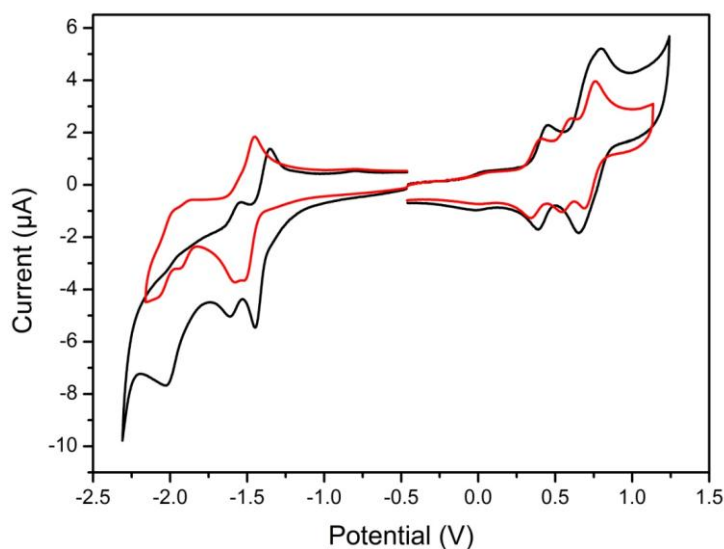


**Figure 4.8.** Cyclic voltammetry of **63** (black) and **64** (red) in solution

The electrochemical study of the triads in the solid state was also carried out, as this is the state in which the materials perform in the active layer of the devices. The oxidation and reduction of **63** and **64** in solid state are shown in Figure 4.9 and Table 4.2 shows all the electrochemical data. Compound **63** shows two irreversible oxidations at +0.64 and +0.79 V. Compound **64** undergoes three overlapping oxidation processes before oxidation of the background occurs at +0.56, +0.64 and +0.75 V. The interpretation of the oxidation waves is the same as in solution. The reduction behaviour of the triads in solid state shows multiple processes. Compound **63** displays five different irreversible reductions at -1.30, -1.34, -1.44, -1.92 and -2.24 V. Compound **64** shows four irreversible peaks at -1.41, -1.49, -1.84 and -2.04 V.

V. The two intense peaks in **63** and **64** can be assigned to the Bodipy and DPP moieties.

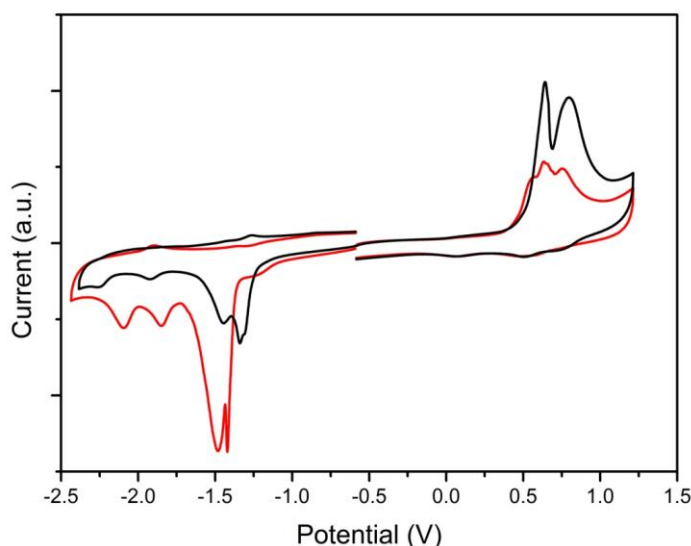


**Figure 4.9.** Cyclic voltammetry of **63** (black) and **64** (red) in solid.

The HOMO and LUMO energy levels were calculated from the onset of the first oxidation and reduction waves and the HOMO-LUMO gap as their difference. Due to the closer interactions between molecules in the solid state, the HOMO-LUMO gap is expected to be lower compared to the HOMO-LUMO gap calculated from the studies in solution. Interestingly, **63** and **64** show higher HOMO-LUMO gaps in the solid state. The film formation stabilises significantly the HOMO level of both triads (see Table 4.2). Although, the HOMO and LUMO energy levels are lower in solid state, the stabilisation of the LUMO is not as large as the HOMO and therefore leads to an increase of the HOMO-LUMO gap. Due to the extended conjugated system, it was also expected to obtain a lower HOMO-LUMO gap for **64**. On the contrary, **63** shows a slightly lower band gap both in solution and in solid state (see Table 4.1 and Table 4.2).

Solution					
	$E_{\text{ox}}/\text{V}$	$E_{\text{red}}/\text{V}$	HOMO/eV	LUMO/eV	HOMO-LUMO gap /eV
<b>63</b>	+0.45/+0.39, <sup>r</sup> +0.80/+0.66 <sup>r</sup>	-1.44/1.34, <sup>qr</sup> -1.61/1.54, <sup>r</sup> -2.01 <sup>ir</sup>	-5.13	-3.50	1.63
<b>64</b>	+0.40/+0.33, <sup>r</sup> +0.60/+0.54, <sup>r</sup> +0.76/+0.69 <sup>r</sup>	-1.51/-1.45, <sup>qr</sup> -1.58/-1.52, <sup>qr</sup> -1.93/-1.87, <sup>qr</sup> -2.09 <sup>ir</sup>	-5.10	-3.40	1.70

**Table 4.1.** Electrochemical behaviour of **63** and **64** in solution

Solid State					
	$E_{\text{ox}}/\text{V}$	$E_{\text{red}}/\text{V}$	HOMO/eV	LUMO/eV	HOMO-LUMO gap /eV
<b>63</b>	+0.64, <sup>ir</sup> +0.79 <sup>ir</sup>	-1.30, <sup>ir</sup> -1.34, <sup>ir</sup> -1.44, <sup>ir</sup> -1.92, <sup>ir</sup> -2.24 <sup>ir</sup>	-5.31	-3.57	1.74
<b>64</b>	+0.56, <sup>ir</sup> +0.64, <sup>ir</sup> +0.75 <sup>ir</sup>	-1.41, <sup>ir</sup> -1.49, <sup>ir</sup> -1.84, <sup>ir</sup> -2.04 <sup>ir</sup>	-5.25	-3.44	1.81

**Table 4.2.** Electrochemical behaviour of **63** and **64** in solid state

The optical properties were characterised by UV-vis absorption spectroscopy. The absorption spectra of triads **63** and **64** in dichloromethane solution and in solid state (a solution of each compound was drop-cast onto ITO) are shown in Figure 4.10 and 4.11, respectively. All the spectra are normalised. For a more complete picture, the absorption spectrum of the di-thieno-DPP (**35**) core in solution is also shown in Figure 4.10. Table 4.3. summarises the optical data.

Both triads **63** and **64** show absorption maxima peaks at 542 nm, which is ascribed to the absorption of the Bodipy units. Interestingly, this value is exactly the same value as the values obtained for a series of Bodipy unit derivatives substituted with oligothiophenes at the *meso* position.<sup>36</sup> Thus, the incorporation of two extra

thiophene rings, and linking to the DPP core, does not affect the absorption peak associated to the Bodipy units. On the other hand, the extension of the  $\pi$ -conjugated system shifts bathochromically the wide absorption associated to the DPP core and thiophene rings. The DPP core substituted with two thiophenes showed two intense peaks at 512 and 548 nm. These peaks are red-shifted 72 and 74 nm respectively for **63** (584 and 622 nm). The shift is even larger for **64** as the conjugation increases (95 and 97 nm) and **64** shows two peaks at 607 and 645 nm. Theoretical calculations support the assignment of these absorption bands to the  $\pi$ - $\pi^*$  transition which is localised on the DPP core (DFT, see next section). Optical HOMO-LUMO gaps in solution were calculated from the onset of the longest wavelength absorption peaks and are summarised in Table 4.3.

The molar absorption coefficient of the triads was also calculated from the absorption ascribed to the Bodipy unit (542 nm). Compound **63** shows a higher absorption ( $\epsilon = 390000 \text{ dm}^3 \text{ mol}^{-1} \text{ cm}^{-1}$ ) than **64** ( $\epsilon = 252000 \text{ dm}^3 \text{ mol}^{-1} \text{ cm}^{-1}$ ). The molar absorption coefficients of triads are considerably higher than the coefficients reported in the literature for the single units (Bodipy substituted on the *meso* position with oligothiophenes<sup>36</sup> and the DPP with oligothiophenes<sup>31</sup>).

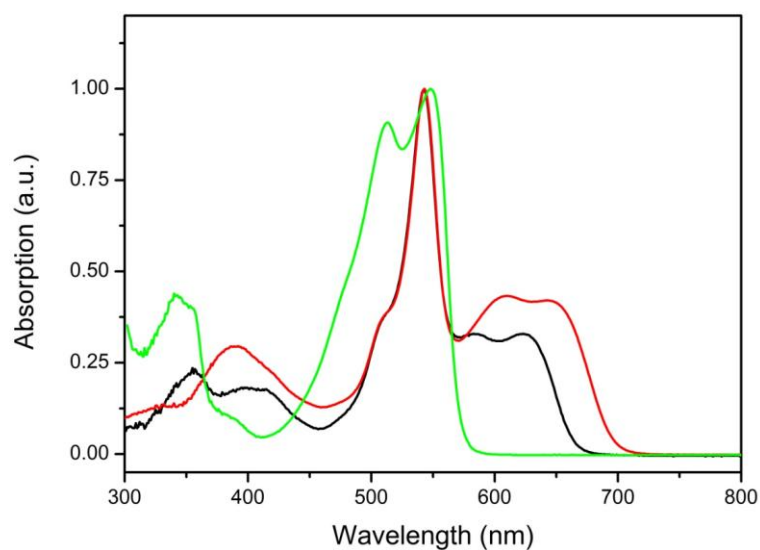


**Figure 4.10.** Normalised UV-vis absorption spectra (for better comparison) of **63** (black), **64** (red) and DPP core (**35**, green) in dichloromethane solution.

In the solid state the triads show the same spectra profile as in solution. In both cases, the main absorption peak occurs at 554 nm. This value is red-shifted 14 nm in comparison with the same peak in solution. Interestingly, the relative intensity of this peak ascribed to the Bodipy unit is diminished. The  $\pi$ - $\pi$  stacking of these compounds in the solid state can affect the HOMO-LUMO transition of the Bodipy and therefore the intensity can decrease. The terthiophene-DPP part of the molecule is also red-shifted. A higher degree of order in the solid state is expected compared to the experiments carried out in solution, which shifts both the absorption wavelength and the HOMO-LUMO gaps towards lower energies. The peaks characteristic of the terthiophene-DPP parts for **63** and **64** appear at 584 and 622 nm and at 607 and 645 nm, respectively. The HOMO-LUMO gaps of the triads were calculated from the onset of the longest wavelength absorption peaks and are summarised in Table 4.3. The onset of **63** shows a small shoulder at lower energy. This absorption (it is not present in solution or in **64**) can be due to aggregation occurring in the solid state. The exact calculation of the HOMO-LUMO gap of **63** is difficult as the onset is diffuse. Nevertheless, the estimated HOMO-LUMO gap of **63** is higher (1.71 eV) compared to the energy gap of **64** (1.67 eV) as the extension of the conjugated system leads to a

lower HOMO-LUMO gap. Interestingly, whereas in solution the HOMO-LUMO gaps of the triads differ significantly (see Table 4.3), in the solid state the incorporation of two extra thiophene rings does not greatly affect to decrease the HOMO-LUMO gap. The possible aggregation of **63** in the solid state can decrease the energy gap making it similar to **64**, even if the conjugation length is shorter.<sup>37</sup>

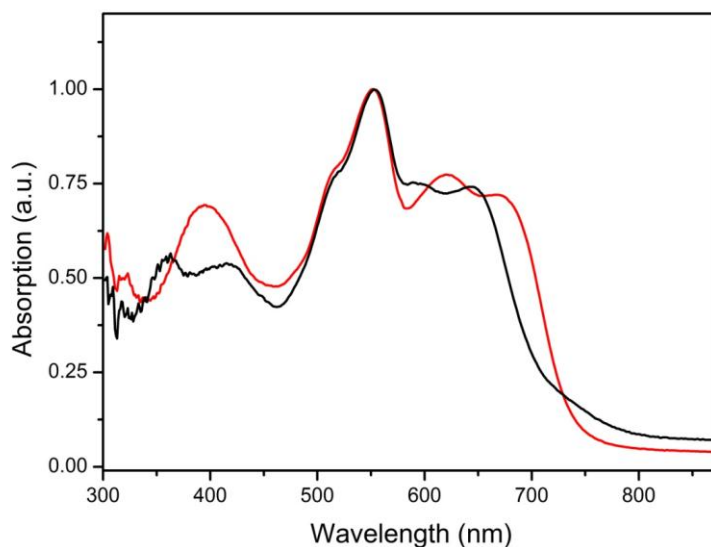


**Figure 4.11.** UV-vis absorption spectra of **63** (black) and **64** (red) core in solid state drop-casted from a dichloromethane on ITO.

	solution			film	
	Absorption peaks / nm	HOMO-LUMO gap / eV	$\epsilon$ $\text{dm}^3 \text{mol}^{-1} \text{cm}^{-1}$	Absorption peaks / nm	HOMO-LUMO gap / eV
<b>63</b>	355, 400 ( <i>br</i> ), 542, 584, 622	1.86	390000	423, 554, 591, 643	1.71
<b>64</b>	386, 542, 607, 645	1.77	252000	395, 554, 619, 668	1.67

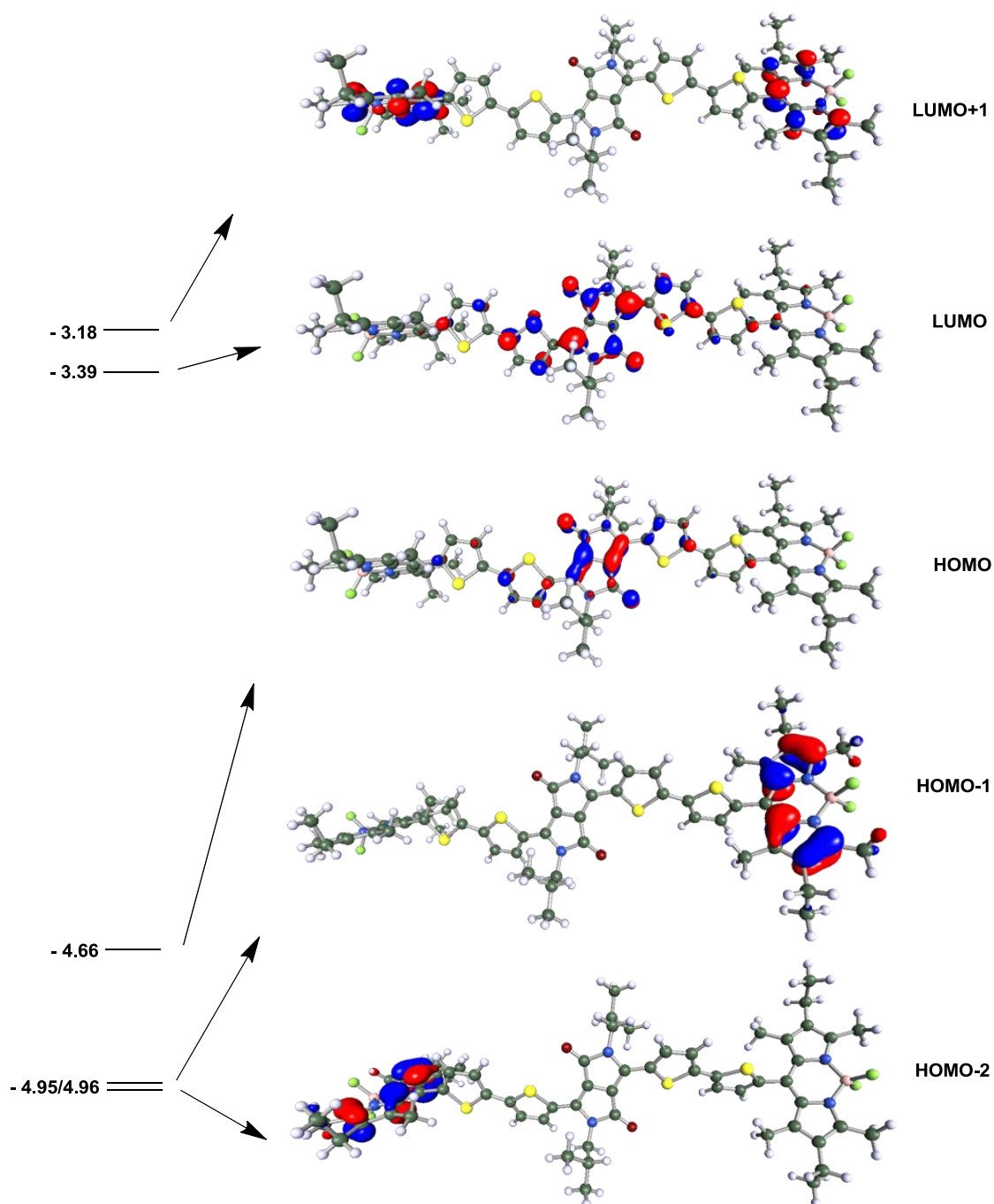
**Table 4.3.** Optical properties of **63** and **64** in solution and solid state

## 4.6. DFT CALCULATIONS

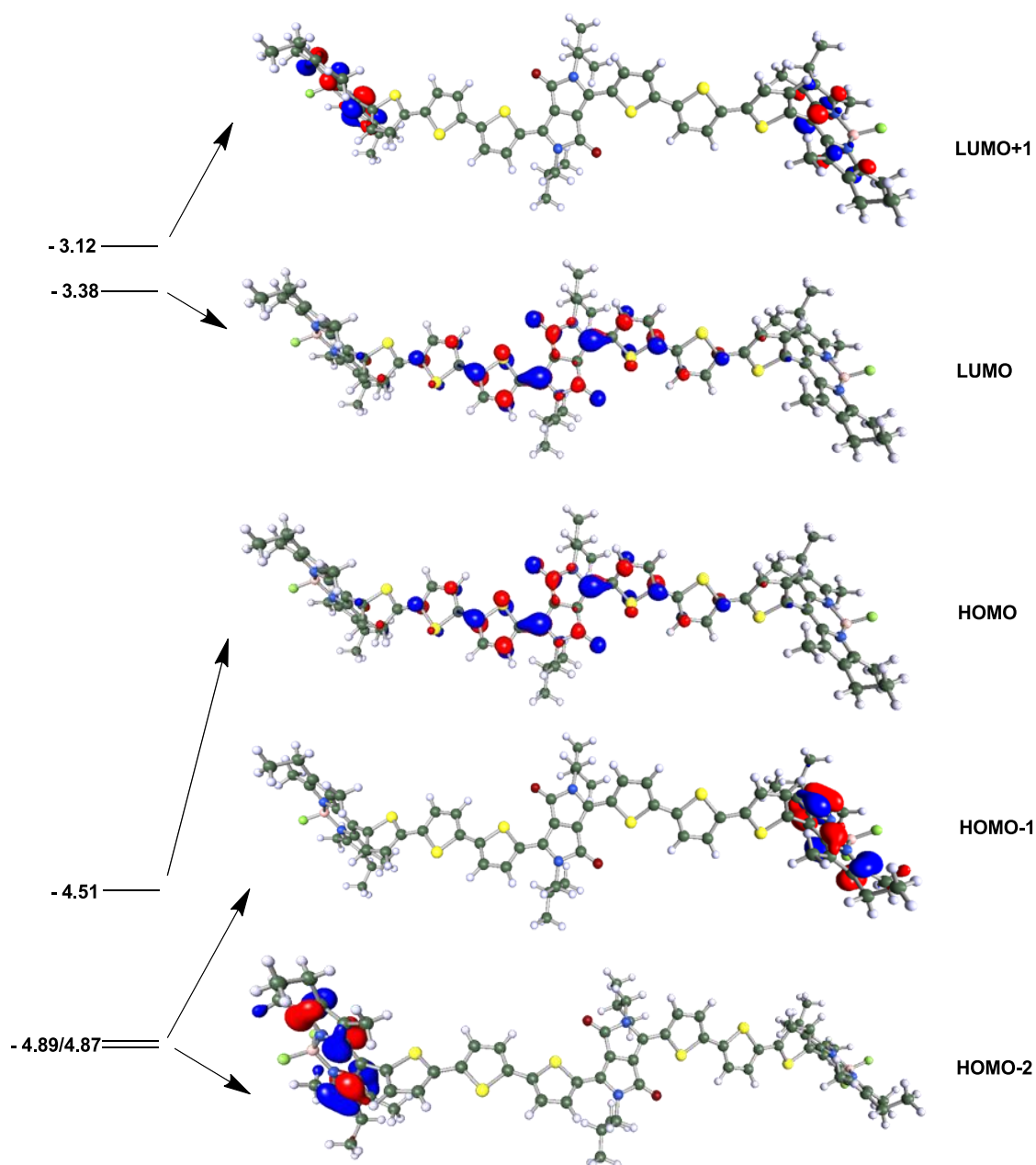
Density functional theory (DFT) calculations of the compounds **63** and **64** were studied in collaboration with Joseph Cameron. The triads were optimised using B97-D functional with def2-TZVP implemented in the TURBOMOLE 6.3.1 programme. In order to decrease computational costs, the long branched aliphatic chains were substituted by *iso*-propyl chains.

Figure 4.12 and Figure 4.13 show the results of the DFT calculations for **63** and **64** respectively. The energy values of the molecular orbitals (MOs) are given in electron-volts. Both compounds show a general trend within the electronic distribution of the Bodipy and DPP units. The HOMO and LUMO of both compounds are localised on the DPP units. However, the higher conjugation present in the terthiophene linker leads to a slightly larger delocalisation of these MOs. As expected, the relative position of the HOMO of **64** is higher than the HOMO of **63**. Due to fact that the LUMO value for both triads is similar, the band gap of **63** is higher than the band gap of **64**.

On the other hand, HOMO-2 and HOMO-1 are localised on the Bodipy units of the molecules. A small symmetry break leads to a slight splitting of the Bodipy MOs. However, from looking at the orbital energies, it can determined that these molecular orbitals are essentially degenerate. The LUMO+1 is also centred on the Bodipy units of the triads.



**Figure 4.12** DFT calculations for **63** (energies are given in electron-volts).



**Figure 4.13** DFT calculations for **64** (energies are given in electron-volts).

## 4.7. CONCLUSIONS AND FUTURE WORK

Two new triads based on two well-known dyes have been synthesised. The triads were obtained *via* Suzuki coupling. The general approach for these compounds was a DPP core linked through thiophene rings to the *meso*-position of a BODIPY derivative. Both compounds were completely characterised. Electrochemical studies showed that these compounds show low band gaps which are usually desirable in materials to be used in OPVs. Additionally, it has been shown by UV-vis absorption spectroscopy that the absorption range of both dyes are complementary. In fact, both triads show large absorption in the full range of UV-visible spectrum.

These compounds have been sent to the group of Professor Ifor D. W. Samuel at School of Physics and Astronomy in the University of St. Andrews in order to investigate the photovoltaic properties of these materials. Preliminary results show that compound **63** exhibits noteworthy behaviour in photon harvesting and an efficiency of  $\approx 1.0\%$  was achieved. These preliminary results are promising and encourage the continued development of these kind of triads. Once all the device work has been carried out and a feed-back of their behaviour is obtained from the physicists, the molecules will be subjected to precise engineering to tune the electronic and the optical properties.

**REFERENCES**

1. G. A. Chamberlain, *Solar Cells*, 1983, **8**, 47-83.
2. C. W. Tang and A. C. Albrecht, *The Journal of Chemical Physics*, 1975, **62**, 2139-2149.
3. C. W. Tang, *Applied Physics Letters*, 1986, **48**, 183-185.
4. N. S. Sariciftci, L. Smilowitz, A. J. Heeger and F. Wudl, *Science*, 1992, **258**, 1474-1476.
5. G. Yu, J. Gao, J. C. Hummelen, F. Wudl and A. J. Heeger, *Science*, 1995, **270**, 1789-1791.
6. Y. Liu, X. Wan, F. Wang, J. Zhou, G. Long, J. Tian, J. You, Y. Yang and Y. Chen, *Advanced Energy Materials*, 2011, **1**, 771-775.
7. V. Steinmann, N. M. Kronenberg, M. R. Lenze, S. M. Graf, D. Hertel, K. Meerholz, H. Bürckstümmer, E. V. Tulyakova and F. Würthner, *Advanced Energy Materials*, 2011, **1**, 888-893.
8. L.-Y. Lin, Y.-H. Chen, Z.-Y. Huang, H.-W. Lin, S.-H. Chou, F. Lin, C.-W. Chen, Y.-H. Liu and K.-T. Wong, *Journal of the American Chemical Society*, 2011, **133**, 15822-15825.
9. J. Zhou, X. Wan, Y. Liu, G. Long, F. Wang, Z. Li, Y. Zuo, C. Li and Y. Chen, *Chemistry of Materials*, 2011, **23**, 4666-4668.
10. Y. Sun, G. C. Welch, W. L. Leong, C. J. Takacs, G. C. Bazan and A. J. Heeger, *Nat Mater*, 2012, **11**, 44-48.
11. A. Mishra and P. Bäuerle, *Angewandte Chemie International Edition*, 2012, **51**, 2020-2067.
12. Y. Lin, Y. Li and X. Zhan, *Chemical Society Reviews*, 2012, **41**, 4245-4272.
13. Y. Li, Q. Guo, Z. Li, J. Pei and W. Tian, *Energy & Environmental Science*, 2010, **3**, 1427-1436.
14. B. Walker, C. Kim and T.-Q. Nguyen, *Chemistry of Materials*, 2010, **23**, 470-482.
15. S. Roquet, A. Cravino, P. Leriche, O. Alévêque, P. Frère and J. Roncali, *Journal of the American Chemical Society*, 2006, **128**, 3459-3466.

16. S. Roquet, R. de Bettignies, P. Leriche, A. Cravino and J. Roncali, *Journal of Materials Chemistry*, 2006, **16**, 3040-3045.
17. C.-Q. Ma, M. Fonrodona, M. C. Schikora, M. M. Wienk, R. A. J. Janssen and P. Bäuerle, *Advanced Functional Materials*, 2008, **18**, 3323-3331.
18. I. A. Wright, A. L. Kanibolotsky, J. Cameron, T. Tuttle, P. J. Skabara, S. J. Coles, C. T. Howells, S. A. J. Thomson, S. Gambino and I. D. W. Samuel, *Angewandte Chemie International Edition*, 2012, **51**, 4562-4567.
19. M. T. Lloyd, A. C. Mayer, A. S. Tayi, A. M. Bowen, T. G. Kasen, D. J. Herman, D. A. Mourey, J. E. Anthony and G. G. Malliaras, *Organic Electronics*, 2006, **7**, 243-248.
20. K. N. Winzenberg, P. Kemppinen, G. Fanchini, M. Bown, G. E. Collis, C. M. Forsyth, K. Hegedus, T. B. Singh and S. E. Watkins, *Chemistry of Materials*, 2009, **21**, 5701-5703.
21. H. Zhou, L. Yang and W. You, *Macromolecules*, 2012, **45**, 607-632.
22. N. M. Kronenberg, V. Steinmann, H. Bürckstümmer, J. Hwang, D. Hertel, F. Würthner and K. Meerholz, *Advanced Materials*, 2010, **22**, 4193-4197.
23. X. Xiao, G. Wei, S. Wang, J. D. Zimmerman, C. K. Renshaw, M. E. Thompson and S. R. Forrest, *Advanced Materials*, 2012, **24**, 1956-1960.
24. J. Mei, K. R. Graham, R. Stalder and J. R. Reynolds, *Organic Letters*, 2010, **12**, 660-663.
25. T. Rousseau, A. Cravino, T. Bura, G. Ulrich, R. Ziessel and J. Roncali, *Chemical Communications*, 2009, 1673-1675.
26. T. Rousseau, A. Cravino, T. Bura, G. Ulrich, R. Ziessel and J. Roncali, *Journal of Materials Chemistry*, 2009, **19**, 2298-2300.
27. T. Rousseau, A. Cravino, E. Ripaud, P. Leriche, S. Rihn, A. De Nicola, R. Ziessel and J. Roncali, *Chemical Communications*, 2010, **46**, 5082-5084.
28. S. Qu and H. Tian, *Chemical Communications*, 2012, **48**, 3039-3051.
29. H. Bronstein, Z. Chen, R. S. Ashraf, W. Zhang, J. Du, J. R. Durrant, P. Shakya Tuladhar, K. Song, S. E. Watkins, Y. Geerts, M. M. Wienk, R. A. J. Janssen, T. Anthopoulos, H. Sirringhaus, M. Heeney and I. McCulloch, *Journal of the American Chemical Society*, 2011, **133**, 3272-3275.

30. A. B. Tamayo, M. Tantiwiwat, B. Walker and T.-Q. Nguyen, *The Journal of Physical Chemistry C*, 2008, **112**, 15543-15552.
31. A. B. Tamayo, B. Walker and T.-Q. Nguyen\*, *The Journal of Physical Chemistry C*, 2008, **112**, 11545-11551.
32. A. B. Tamayo, X.-D. Dang, B. Walker, J. Seo, T. Kent and T.-Q. Nguyen, *Applied Physics Letters*, 2009, **94**, 103301.
33. B. Walker, A. B. Tamayo, X.-D. Dang, P. Zalar, J. H. Seo, A. Garcia, M. Tantiwiwat and T.-Q. Nguyen, *Advanced Functional Materials*, 2009, **19**, 3063-3069.
34. D. Hablot, P. Retailleau and R. Ziessel, *Chemistry – A European Journal*, 2010, **16**, 13346-13351.
35. D. Hablot, A. Harriman and R. Ziessel, *Angewandte Chemie International Edition*, 2011, **50**, 7833-7836.
36. A. C. Benniston, G. Copley, A. Harriman and R. Ryan, *Journal of Materials Chemistry*, 2011, **21**, 2601-2608.
37. J. Roncali, *Chemical Reviews*, 1997, **97**, 173-206.